Formation of large coronary arteries by cardiac progenitor cells

Jochen Tillmanns*, Marcello Rota*, Toru Hosoda*, Yu Misao*, Grazia Esposito*, Arantxa Gonzalez*, Serena Vitale*, Carola Parolin*, Saori Yasuzawa-Amano*, John Muraski*, Antonella De Angelis*, Nicole LeCapitaine*, Robert W. Siggins*, Maria Loredo*, Claudia Bearzi*, Roberto Bolli†, Konrad Urbanek*, Annarosa Leri*, Jan Kajstura*, and Piero Anversa*‡

*Cardiovascular Research Institute, Department of Medicine, New York Medical College, Valhalla, NY 10595; and †Institute of Molecular Cardiology, University of Louisville, Louisville, KY 40292

Coronary artery disease is the most common cause of cardiac failure in the Western world, and to date there is no alternative to bypass surgery for severe coronary atherosclerosis. We report that c-kit-positive cardiac progenitor cells (CPCs) activated with insulin-like growth factor 1 and hepatocyte growth factor before their injection in proximity of the site of occlusion of the left coronary artery in rats, engrafted within the host myocardium forming temporary niches. Subsequently, CPCs divided and differentiated into endothelial cells and smooth muscle cells and, to a lesser extent, into cardiomyocytes. The acquisition of vascular lineages appeared to be mediated by the up-regulation of hypoxia-inducible factor 1α, which promoted the synthesis and secretion of stromal-derived factor 1 from hypoxic coronary vessels. Stromal-derived factor 1 was critical in the conversion of CPCs to the vascular fate. CPCs formed conductive and intermediate-sized coronary arteries together with resistance arterioles and capillaries. The new vessels were connected with the primary coronary circulation, and this increase in vascularization more than doubled myocardial blood flow in the infarcted myocardium. This beneficial effect, together with myocardial regeneration attenuated postinfarction dilated myopathy, reduced infarct size and improved function. In conclusion, locally delivered activated CPCs generate de novo coronary vasculature and may be implemented clinically for restoration of blood supply to the ischemic myocardium.

coronary blood flow | infarct size | myocardial regeneration | stem cells | vasculogenesis

Alteration in the balance between oxygen demand and supply has been viewed as the critical determinant of ischemic cardiomyopathy in humans (1, 2). The etiology of ischemic myocardial injury is represented by lesions of the major epicardial coronary arteries that restrict blood flow to the distal myocardium leading to infarction and scar formation. Coronary artery disease (CAD) is the most common cause of cardiac failure and accounts for 500,000 cases of bypass surgery per year in the United States alone. To date there is no alternative to bypass surgery for severe coronary atherosclerosis, which increases with age and dramatically affects the elderly population (1, 2). Regeneration of coronary arteries would change dramatically the goal of cell therapy for the ischemic heart. Prevention of myocardial injury would become the end point of cell therapy rather than the partial repair of established damage.

The adult heart contains a population of c-kit-positive cardiac progenitor cells (CPCs), which are self-renewing, clonogenic, and multipotent *in vitro* and regenerate infarcted myocardium *in vivo* (3, 4). Additionally, CPCs possess the hepatocyte growth factor (HGF) c-Met receptor system (HGF–c-Met) and the insulin-like growth factor 1 (IGF-1)–IGF-1 receptor (IGF-1R) system (IGF-1–IGF-1R). The HGF–c-Met modulates predominantly CPC migration, and the IGF-1–IGF-1R modulates primarily CPC division and survival (4, 5). These observations formed the basis of the present study, in which we report that CPCs activated *in vitro* with IGF-1 and HGF before their delivery *in vivo* have the potential to

reconstitute the various portions of the coronary circulation in the infarcted rat heart. This increase in vascularization has multiple beneficial effects; it improves myocardial blood flow, attenuates the development of the postinfarction myopathy, reduces infarct size, and enhances ventricular function.

Results

CPC Survival and Engraftment. Injection of clonogenic CPCs (nonactivated CPCs) or clonogenic CPCs, activated with HGF and IGF-1 (activated CPCs) before their implantation in proximity of the occluded left coronary artery, had different consequences on cell homing, growth, and differentiation. Both cell populations expressed EGFP, which was used as a marker of the progeny of the transplanted cells in the recipient heart. Activated and nonactivated CPCs accumulated within the nondamaged myocardium at the site of injection (Fig. 1*A*). However, nonactivated CPCs showed a high apoptotic rate [see supporting information (SI) Fig. 6] and a modest level of cell proliferation (Fig. 1*B*); apoptosis increased from 12 to 24 to 48 h, leading to a complete disappearance of the implanted cells in 2 weeks. Activated CPCs behaved differently; at 12 h the rate of apoptosis was similar to the rate of cell replication but at 24 and 48 h cell division exceeded cell death (Fig. 1*C* and SI Fig. 6). An important aspect of cell survival and growth is cell engraftment; engraftment requires the synthesis of proteins that establish cell-to-cell contact and the interaction between cells and the extracellular matrix (6). The presence of connexin and cadherins in CPCs and adjacent cells was used as a criterion of cell engraftment. Connexin 43, N- and E-cadherin were expressed in a large fraction of activated CPCs (38 ± 12%) and were rarely seen in nonactivated cells (3.8 ± 3.1%). These proteins were found between CPCs and between CPCs and myocytes or fibroblasts (Fig. 1 *D–G*); myocytes and fibroblasts function as supporting cells in CPC niches (7).

Apoptosis was restricted to nonengrafted cells that did not express connexin 43 (Fig. 1*H*), E-cadherin, and N-cadherin; it was never detected in engrafted cells expressing junctional and adhesion proteins. This phenomenon is consistent with anoikis of the nonengrafted cells, which is one of the aspects of programmed cell death triggered by the lack of cell-to-cell contacts (8). Quantitative measurements at 2 days showed that

Fig. 1. Engraftment of CPCs. (*A*) Site of injection of activated EGFP-positive CPCs (green) 24 h after infarction. (*B* and *C*) Apoptosis and proliferation in nonactivated and activated CPCs. (*D–G*) Connexin 43 (Cx43, yellow) and E-cadherin (E-cadh, yellow) are expressed between activated CPCs and myocytes (*D*, α-SA, white; *D Inset*, arrowheads) and between CPCs and fibroblasts (*F*, procollagen, red; *F Inset*, arrowhead). (*E* and *G*) Positive controls: cardiomyocytes and coronary vessel. (*H*) Apoptotic nonactivated CPCs (magenta, arrows) do not express Cx43 (yellow, arrowheads). (*I*) Site of injection of activated EGFP-positive CPCs 1 month after implantation in intact myocardium. CPCs do not express α-SA (red); only a small fraction of cells is positive for α-SMA (magenta, arrowheads) and VWF (yellow, arrowhead). The arrow points to the mitotic image.

only ≈5% (4,800 ± 2,600) of the 80,000–100,000 injected nonactivated CPCs were present in the myocardium whereas ≈50% (48,000 ± 18,000) of activated CPCs were detected. These values are the product of three variables: cellular engraftment, death, and division.

To strengthen the possibility that activation of CPCs by growth factors (GFs) played a role in cell engraftment, activated CPCs were injected in the intact myocardium of noninfarcted rats. One month later, a large quantity of cells was present at the site of injection in the epicardial region of the heart (Fig. 1*I*). The implanted cells were small and negative for α-sarcomeric actin (α-SA) and procollagen; 4% of EGFP-positive cells expressed α-smooth muscle actin (α-SMA) and 2% von Willebrand factor (VWF). The modest lineage commitment of CPCs was most likely related to the absence of tissue damage (3, 9, 10). Apoptosis (0.67 ± 0.29%) and cell division (0.84 ± 0.35%) were minimal at this time; the engrafted cells expressed connexin 43, N-cadherin, and E-cadherin (SI Fig. 7).

CPC Adaptation to Ischemia. The question was then whether changes in the cardiac microenvironment created by coronary occlusion influenced the differentiation of CPCs into vascular smooth muscle cells (SMCs) and endothelial cells (ECs), leading to the formation of coronary vessels. Potential candidates include the hypoxia-inducible factor 1α (HIF-1α), which is a transcriptional regulator of the stromal-derived factor 1 (SDF-1) chemokine (11). HIF-1α and SDF-1 are up-regulated with ischemia and correlate with the oxygen gradient within the tissue (11, 12). In the absence of cell injection, the expression of HIF-1α and SDF-1 increased significantly after infarction below the ligature, at the border of the infarct, and within the infarct (Fig. 2*A* and SI Fig. 8). HIF-1α was detected in myocyte, EC, and SMC nuclei whereas SDF-1 was restricted to ECs and SMCs within the wall of coronary vessels (Fig. 2*B* and SI Fig. 8). The percentage of ECs and SMCs positive for HIF-1α and SDF-1 and the percentage of myocytes positive for HIF-1α increased from 1 to 6 h and remained elevated at 12 h (SI Fig. 9).

At 6–12 h the concentration of HGF and IGF-1 remained constant in the various regions of the infarcted heart (Fig. 2*C*). To characterize further the effects of IGF-1 and HGF on CPCs, these cells were stimulated *in vitro* with GFs and the expression of HIF-1α and the synthesis of SDF-1 were determined. There was up-regulation of HIF-1α mRNA and protein together with enhanced formation of SDF-1 (Fig. 2 *D–F* and SI Fig. 10).

To establish whether the effects of GFs on HIF-1α and SDF-1 were mediated by activation of the PI3K/Akt pathway, nonactivated and activated CPCs were exposed to an inhibitor of Akt phosphorylation. In both cases, the expression of phospho-Akt in CPCs decreased markedly (Fig. 3*A*). Similarly, HIF-1α expression was clearly attenuated. Additionally, the synthesis of SDF-1 was decreased significantly in both cell classes. These findings point to the critical role that IGF-1–HGF and the PI3K/Akt pathway may have in the survival and engraftment of CPCs on one hand and HIF-1α and SDF-1 expression on the other hand (13, 14).

To test whether the formation of SDF-1 by ECs and the interaction of ECs with CPCs promote the commitment of CPCs into vascular cells, *in vitro* studies were performed. Activated and nonactivated CPCs were cocultured with human umbilical vein endothelial cells (HUVECs) under normoxic and hypoxic conditions. CPCs express CXCR4, the receptor of SDF-1 (Fig. 3*B* and SI Fig. 10). At baseline, HUVECs showed low degrees of HIF-1α, and hypoxia markedly up-regulated its expression (Fig. 3*C*). In normoxia, the coculture of HUVECs with CPCs enhanced the commitment of activated and non-
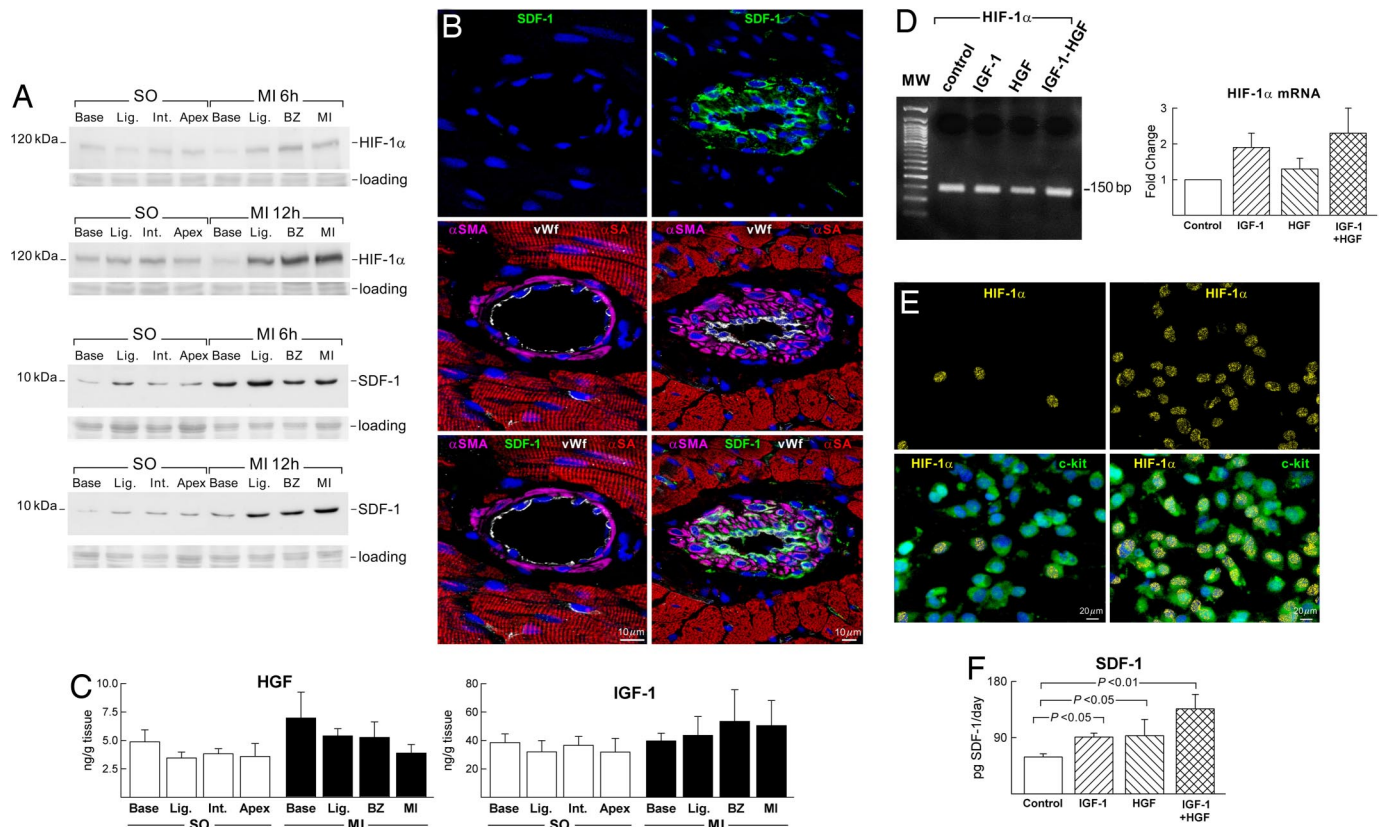
MEDICAL SCIENCES

Fig. 2. Ischemia, HIF-1α, and SDF-1. (*A*) HIF-1α and SDF-1 are up-regulated after infarction [see SI Fig. 8 *A* and *B* (for sampling and for OD, respectively)]. MI, myocardial infarct; SO, sham-operated. (*B*) SDF-1 was negligible in resistance arterioles above the ligature (*Left*) but was highly expressed in arterioles located below the ligature (*Right*). (*Middle*) Myocytes (α-SA, red), ECs (VWF, white), and SMCs (α-SMA, magenta). (*C*) HGF and IGF-1 in the myocardium by ELISA. (*D*) Real-time RT-PCR of HIF-1α in CPCs exposed to IGF-1, HGF, and IGF-1–HGF. Control, CPCs not treated with IGF-1 or HGF. Nucleotide sequences are in SI Fig. 10. (*E*) HIF-1α (yellow) is rarely present in CPCs (c-kit, green) in the absence of IGF-1 and HGF (*Left*) whereas HIF-1α is detected in numerous CPCs exposed to IGF-1–HGF (*Right*). Colocalization of HIF-1α and c-kit is shown in *Lower*. (*F*) SDF-1 levels in CPCs by ELISA at baseline and after IGF-1 and/or HGF stimulation.

activated CPCs to SMCs and ECs (Fig. 3*D*). Myocyte formation was not affected. With hypoxia, nonactivated and activated CPCs cocultured with HUVECs showed a potentiated response; they acquired predominantly the EC and SMC phenotype and, to a lesser extent, the cardiomyogenic fate. Activated CPCs, however, exhibited a much higher level of proliferation (Fig. 3*D*). The specificity of CXCR4 activation was documented by inhibiting this receptor with neutralizing antibody.

To establish whether up-regulation of HIF-1α in ECs is a critical factor in CPC differentiation, HUVECs were transfected with siRNA against HIF-1α and cocultured with nonactivated and activated CPCs. This strategy decreased dramatically the expression of HIF-1α in HUVECs. Importantly, the fraction of GATA6-positive and Ets1-positive nonactivated and activated CPCs decreased markedly (Fig. 3*E*). In the absence of HUVECs, the addition of SDF-1 to normoxic cultures of nonactivated and activated CPCs induced cell division and increased in a comparable manner EC and SMC formation and to a limited degree myocyte differentiation (Fig. 3*F*). Transcripts for VWF, myosin heavy chain 11 (Mhc11), and myosin light chain 2v (Mlc2v), indicative, respectively, of EC, SMC, and myocyte differentiation, followed a similar pattern (Fig. 3*G* and SI Fig. 10). Thus, CPC activation by hypoxia and/or SDF-1 favors the generation of ECs and SMCs.

Formation of Coronary Arteries. The effects of activated CPCs on the development of conductive coronary arteries and their branches

were evaluated at 2 weeks and at 1 month. At 2 weeks, newly formed EGFP-positive coronary arteries with a diameter up to 250 μm were found in the epimyocardium adjacent to the site of injection (Fig. 4*A* and SI Fig. 11). Vessels with a diameter >64 μm were restricted to the viable myocardium of the base and upper midregion of the ventricle (Fig. 4*B*). They were not present in the scarred myocardium at 2 weeks. However, newly formed resistance arterioles were predominantly located in the infarct (Fig. 4*C*). Arterioles with a diameter <25 μm were limited to the infarct and were not detected in the spared myocardium. A few capillaries were also present but mostly within the infarct. These observations provide evidence for a selective response of CPCs to the regional needs of the organ, which appear to condition stem cell behavior (15, 16). In all cases, the wall of large, intermediate, and small coronary arteries and capillaries was composed of EGFP-positive SMCs and ECs. Vasculogenesis seemed to be the only mechanism of vessel growth.

To determine whether the formed coronary vasculature represented temporary vessels that subsequently atrophied or functionally competent vessels that grew further with time, we extended our observations to 1 month. At this interval, numerous EGFP-positive coronary vessels with diameters ranging from 6 to 250 μm were present in both the infarct and viable myocardium, suggesting that time resulted in an expansion of the coronary vasculature. Large, intermediate, and small coronary arteries and arterioles together with capillary profiles were detected in both regions of the infarcted heart (SI Figs. 12 and 13). As at 2 weeks, the regenerated vessels were composed only of EGFP-positive SMCs and ECs. This possibility was strengthened by the detection of the DNA sequence
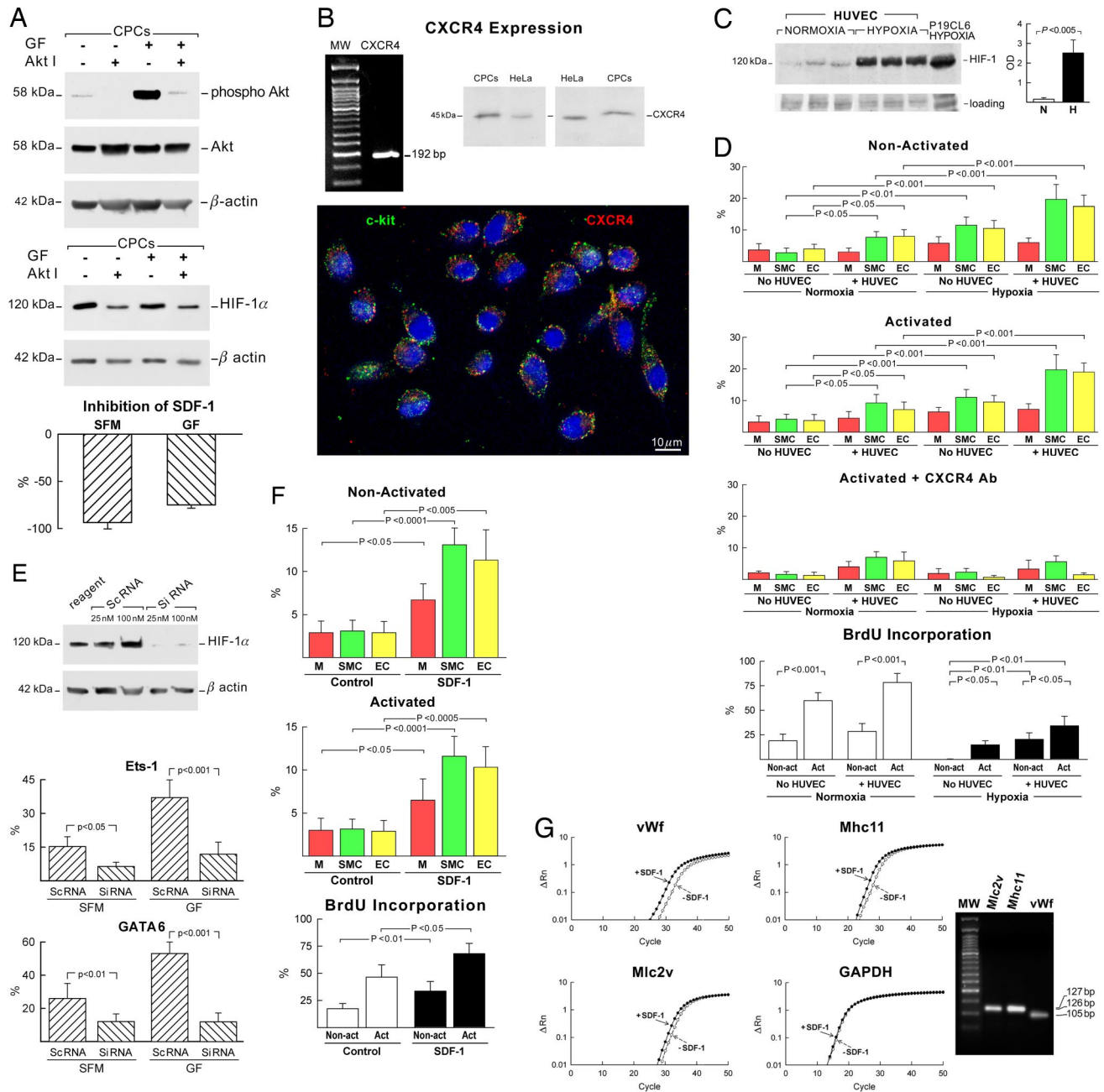
Fig. 3. Hypoxia, SDF-1, and CPC differentiation. (*A*) Akt inhibition (Akt I) of nonactivated and activated CPCs decreased the expression of phospho-Akt, HIF-1α (56% decrease in controls and 44% decrease in GF-treated CPCs), and SDF-1 synthesis. (*B*) CPCs express CXCR4 at the mRNA and protein levels. The presence of CXCR4 (red) in CPCs was confirmed by immunocytochemistry. (*C*) Hypoxia up-regulates 16-fold HIF-1α expression in HUVECs. P19CL6 cells were used as positive control. (*D*) Differentiation and proliferation of nonactivated and activated CPCs. Exposure of activated CPCs to CXCR4 antibody attenuates differentiation in the presence of hypoxia. (*E*) Expression of HIF-1α in HUVECs transfected with HIF-1α siRNA. When CPCs are cocultured with transfected HUVECs, the differentiation of CPCs into vascular cells decreased as documented by immunocytochemistry. (*F*) SDF-1 favors CPC differentiation. (*G*) SDF-1 up-regulates VWF, Mhc11, and Mlc2v in CPCs. Nucleotide sequences are in SI Fig. 10.

of EGFP by PCR in treated infarcted hearts (Fig. 4*D* and SI Fig. 14). Quantitative results documented that all classes of coronary vessels had developed or expanded from 2 weeks to 1 month (Fig. 4*E*).

To assess whether the reconstitution of coronary vessels involved fusion events, the formation of heterokaryons was established by measuring the number of sex chromosomes in nuclei of EGFP-positive ECs and SMCs within the vessel wall (5, 17). Because female clonogenic activated CPCs were implanted in female hearts, the number of X chromosomes was identified by FISH (Fig. 4 *F* and *G* and SI Fig. 15). Sixty-four

vessels were examined in five animals; this magnitude of sampling accounted for nearly 2,000 EC and SMC nuclei. In all cases, at most two X chromosomes were found in EC and SMC nuclei, suggesting that cell fusion played a minor role in the restoration of the coronary vasculature by activated CPCs.

To determine whether new coronary vessels were connected with the aorta and the existing coronary circulation, an *ex vivo* preparation was used. The heart was perfused through the aorta with rhodamine-labeled dextran. This molecule does not cross the endothelium, and it allows the visualization of the

MEDICAL SCIENCES

Fig. 4. Vessel regeneration. (*A*) Epimyocardium of an infarcted treated heart at 2 weeks: three new coronary arteries (*Upper*, EGFP, green) are present in the spared myocardium (SM) and border zone (BZ)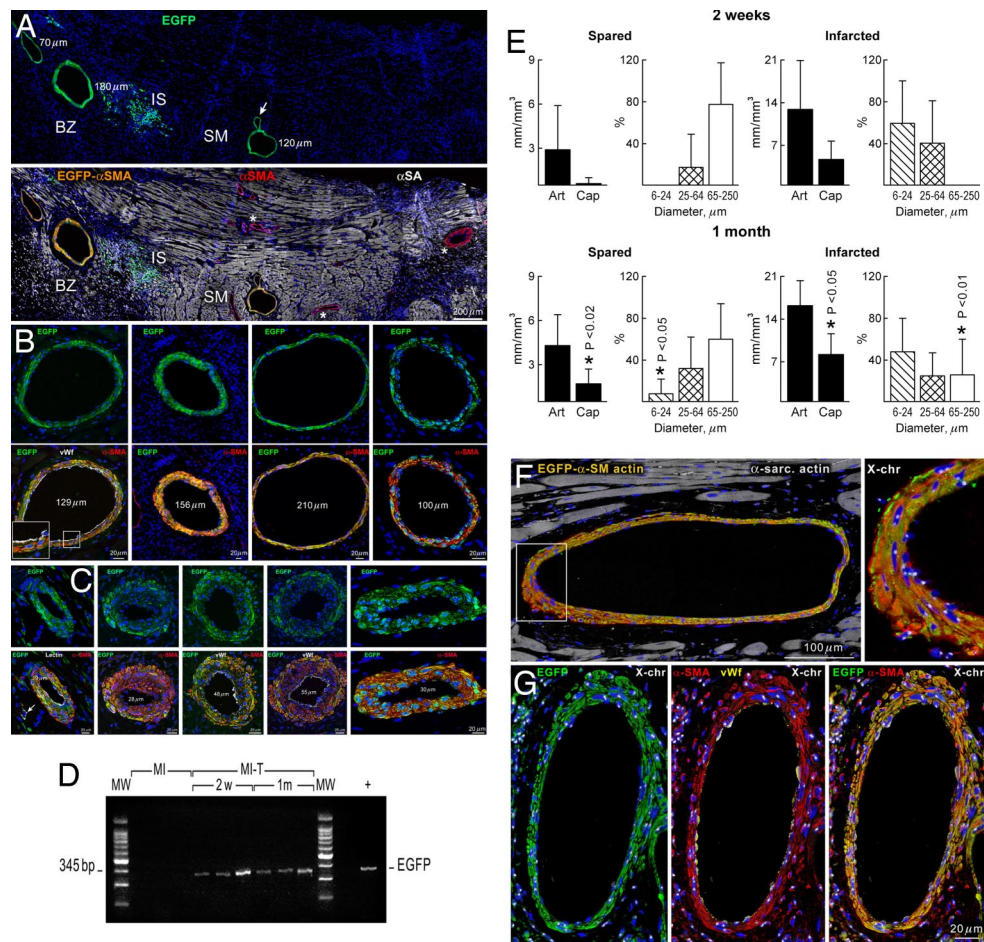. The arrow points to a branching vessel. Colocalization of EGFP and αSMA is shown (*Lower*, orange). Preexisting coronary branches are EGFP-negative (*Upper*) and α-SMA-positive (*Lower*, red, asterisks). A cluster of EGFP-positive cells is present at the injection site (IS). Myocytes, α-SA: white. (*B*) Large regenerated arteries (*Upper*, EGFP, green) in spared myocardium at 2 weeks. Colocalization of EGFP and α-SMA is shown (*Lower*, orange). *Inset* illustrates ECs (VWF, white). (*C*) Infarct with regenerated intermediate and small coronary arteries. In three panels in *Lower* ECs are labeled by lectin or VWF (white). The leftmost panel in *Lower* shows one capillary (arrow). (*D*) EGFP DNA in infarcted treated hearts (MI-T) at 2 weeks and at 1 month. MI, untreated infarcted hearts. Peripheral blood from EGFP transgenic mice was used as positive control (+). Nucleotide sequences are in SI Fig. 13. (*E*) Vessel formation. Solid bars (Art) correspond to the regeneration of arteries in the spared and infarcted myocardium. The luminal diameters of the regenerated arteries are shown in the adjacent panels. ∗, Different vs. 2 weeks. (*F* and *G*) SMCs and ECs in regenerated large coronary arteries exhibit at most two X chromosomes. In *G* the colocalization of EGFP (green), α-SMA (red), VWF (yellow), and X chromosomes (white dots) is shown separately and merged together. The area included in the rectangle in *F* is shown at a higher magnification in *Inset*.

coronary vasculature by two-photon microscopy (5, 17). Resident and generated coronary vessels were distinguished, respectively, by the absence and presence of EGFP labeling of the wall. Collagen was detected by second harmonic generation (18). A discrete localization of collagen corresponded to viable myocardium whereas extensive accumulation of collagen reflected infarcted myocardium (SI Fig. 16). By this approach, the red fluorescence of rhodamine-labeled dextran, the green fluorescence of EGFP, and the blue fluorescence of collagen were detected directly in the nonfixed infarcted heart in the absence of immunolabeling (19).

Large coronary arteries and their branches were identified within the noninfarcted epimyocardium of treated rats at 2 weeks (Fig. 5*A*). These vessels had EGFP-positive walls that were surrounded by minimal amounts of collagen. Similar vessels were found in the border zone and in the scarred myocardium at 2 weeks and at 1 month (SI Fig. 17). When resolution permitted, a direct connection was recognized between preexisting and generated coronary vessels (Fig. 5*B*). These findings documented the integration of temporally distinct, old and new, segments of the coronary vasculature. Measurements of coronary blood flow with nonradioactive microspheres were then obtained. In comparison with untreated infarcts, myocardial perfusion was 2.5-fold higher in treated infarcts at 1 month (Fig. 5*C*).

At times the new coronary vessels traversed the epicardial region of the infarct where they were surrounded by extensive foci of newly formed EGFP-positive myocytes (Fig. 5*D*). The regeneration of infarcted myocardium was detected first in the region proximal to the ligature and the site of injection of the activated CPCs. From 2 weeks to 1 month, myocardial regeneration extended toward the mid-region of the infarct and began to invade the apical portion of the heart (SI Fig. 17). Cardiac repair reduced infarct size at the base of the heart by 12% and 38% at 2 weeks and at 1 month, respectively. Smaller decreases were detected in the mid-region and apex (Fig. 5*E*). The improvement in coronary circulation together with myocardial reconstitution led to attenuation of ventricular dilation and to an increase in wall thickness-to-chamber radius ratio and ventricular mass-to-chamber volume ratio (SI Fig. 18). Importantly, cell therapy reduced the hemodynamic alterations in left ventricular end-diastolic pressure, developed pressure, positive and negative dP/dt, and diastolic wall stress (Fig. 5*F*).

Discussion

During development, endothelial and hematopoietic cells arise from a common progenitor, the hemangioblast (20). The endothelial differentiation of hemangioblasts, however, was considered restricted to the embryo, and the possibility of vasculogenesis in adulthood was questioned. The identification of circulating endothelial progenitor cells (EPCs) and the documentation of their ability to transdifferentiate into SMCs and form arterioles and capillaries in the peripheral circulation (21, 22), and potentially in the infarcted human heart (23), have introduced a novel perspective for the treatment of CAD. Other subsets of bone marrow cells have also been shown to promote vasculogenesis in the heart (24) and damaged organs (25).

We report that activated CPCs regenerate conductive, intermediate-sized and small coronary arteries and arterioles together with capillary structures *in vivo*, replacing partly the

Fig. 5. Newly formed coronary vessels are functionally competent. (*A*) Large coronary artery and its branches located in the viable myocardium of a treated rat contain rhodamine-labeled dextran (Rh-D, red) and possess EGFP-positive wall (green). Coll, collagen (blue). (*B*) Functional integration of newly formed vessels (EGFP-positive wall, green) with resident vessels (EGFP-negative wall). The white circles delimit the sites of anastomosis. (*C*) Coronary blood flow in untreated (MI) and treated (MI-T) infarcts. SO, sham-operated. (*D*) The new vessel and its branches are surrounded by EGFP-positive cells within the infarct. EGFP-positive cells (green) correspond to newly formed myocytes (*Lower*, α-SA, red). (*E*) Myocardial regeneration in the apex, mid-portion of the left ventricle (MP), and base is shown quantitatively. (*F*) Cardiac function. Left ventricular end-diastolic pressure (LVEDP), LV developed pressure (LVDP), positive and negative dP/dt, and diastolic wall stress improved in treated rats.

function of the occluded coronary artery and its distal branches. This unprecedented degree of vasculogenesis improves myocardial perfusion and positively interferes with the development of the postinfarction myopathy. Blood flow to the myocardium can be enhanced only by formation of arteries and arterioles whereas capillaries control oxygen diffusion but have no influence on flow regulation (26). The documentation that undifferentiated cells with angiogenic properties reside in the heart questions the bone marrow as the exclusive reservoir or source of stem cells for therapeutic angiogenesis. Moreover, there is no evidence that EPCs or bone marrow cell subsets can form large conductive arteries pointing to activated CPCs as the cell of choice for biological coronary bypass.

The pharmacological and surgical management of patients affected by CAD has improved significantly in the last three decades (1), but, despite these advances, morbidity and mortality for ischemic cardiomyopathy continue to increase and parallel the extension in median lifespan of the population (27). The inevitable small number of surgical grafts that can be performed, the possibility of restenosis of the grafted vessels, and the complexity of reintervention in high-risk patients (28) emphasize the need for the development of new strategies for the management of CAD. Moreover, cardiac transplantation for end-stage ischemic cardiomyopathy has age restriction and is limited by the small number of donor hearts.

Our observations suggest that CPCs possess a significant degree of plasticity and that the formation of a committed progeny is conditioned by the etiology of the tissue injury and/or the needs of the damaged organ (15, 16). When CPCs are implanted in proximity of an acute infarct, they sense signals that ultimately lead to tissue regeneration (3, 4). However, as shown here, CPCs delivered in proximity of an occluded coronary artery are influenced by signals transmitted from the hypoxic ECs, which, in the end, result in the restoration of various segments of the coronary vasculature. Importantly, caution has to be exercised in the interpretation of our data because the long-term outcome of this type of cell therapy remains unknown. Additionally, studies in large animals will have to be performed to carefully characterize the effects of CPCs on the physiology of the coronary circulation.

Materials and Methods

CPCs used in these studies were isolated from female Fischer 344 rats. A single clonogenic c-*kit*-positive CPC expressing EGFP was used to develop an EGFP-positive, c-*kit*-positive CPC clone (see *SI Materials and Methods*).

1. McMurray JJV, Pfeffer MA (2005) *Lancet* 365:1877–1889.
2. Neubauer S (2007) *N Engl J Med* 356:1140–1151.
3. Beltrami AP, Barlucchi L, Torella D, Baker M, Limana F, Chimenti S, Kasahara H, Rota M, Musso E, Urbanek K, et al. (2003) *Cell* 114:763–766.
4. Linke A, Muller P, Nurzynska D, Casarsa C, Torella D, Nascimbene A, Castaldo C, Cascapera S, Bohm M, Quaini F, et al. (2005) *Proc Natl Acad Sci USA* 102:8966–8971.
5. Urbanek K, Rota M, Cascapera S, Bearzi C, Nascimbene A, De Angelis A, Hosoda T, Chimenti S, Baker M, Limana F, et al. (2005) *Circ Res* 97:663–673.
6. Lapidot T, Dar A, Kollet O (2005) *Blood* 106:1901–1910.
7. Urbanek K, Cesselli D, Rota M, Nascimbene A, De Angelis A, Hosoda T, Bearzi C, Boni A, Bolli R, Kajstura J, et al. (2006) *Proc Natl Acad Sci USA* 103:9226–9231.
8. Valentijn AJ, Zouq N (2004) *Biochem Soc Trans* 32:421–425.
9. Oh H, Bradfute SB, Gallardo TD, Nakamura T, Gaussin V, Mishina Y, Pocius J, Michael LH, Behringer RR, Garry DJ, et al. (2003) *Proc Natl Acad Sci USA* 100:12313–12318.
10. Mouquet F, Pfister O, Jain M, Oikonomopoulos A, Ngoy S, Summer R, Fine A, Liao R (2005) *Circ Res* 97:1090–1092.
11. Ceradini DJ, Kulkarni AR, Callaghan MJ, Tepper OM, Bastidas N, Kleinman ME, Capla JM, Galiano RD, Levine JP, Gurtner GC (2004) *Nat Med* 10:858–864.
12. Abbott JD, Huang Y, Liu D, Hickey R, Krause DS, Giordano FJ (2004) *Circulation* 110:3300–3305.
13. Fukuda R, Hirota K, Fan F, Jung YD, Ellis LM, Semenza GL (2002) *J Biol Chem* 277:38205–38211.
14. Tacchini L, De Ponti C, Matteucci E, Follis R, Desiderio MA (2004) *Carcinogenesis* 25:2089–2100.
15. Korbling M, Estrov Z (2003) *N Engl J Med* 349:570–582.
16. Scadden DT (2006) *Nature* 441:1075–1079.
17. Dawn B, Stein AB, Urbanek K, Rota M, Whang B, Rastaldo R, Torella D, Tang XL, Rezazadeh A, Kajstura J, et al. (2005) *Proc Natl Acad Sci USA* 102:3766–3771.
18. Schenke-Layland K, Riemann I, Stock UA, Konig K (2005) *J Biomed Opt* 10:024017-1–024017-5.
19. Helmchen F, Fee MS, Tank DW, Denk W (2001) *Neuron* 31:903–912.
20. Coultas L, Chawengsaksophak K, Rossant J (2005) *Nature* 438:937–945.
21. Asahara T, Murohara T, Sullivan A, Silver M, van der Zee R, Li T, Witzenbichler B, Schatteman G, Isner JM (1997) *Science* 275:964–967.
22. Aicher A, Heeschen C, Mildner-Rihm C, Urbich C, Ihling C, Technau-Ihling K, Zeiher AM, Dimmeler S (2003) *Nat Med* 9:1370–1376.
23. Schachinger V, Erbs S, Elsasser A, Haberbosch W, Hambrecht R, Holschermann H, Yu J, Corti R, Mathey DG, Hamm CW, et al. (2006) *N Engl J Med* 355:1210–1221.
24. Yoon YS, Wecker A, Heyd L, Park JS, Tkebuchava T, Kusano K, Hanley A, Scadova H, Qin G, Cha DH, et al. (2005) *J Clin Invest* 115:326–338.
25. Losordo DW, Dimmeler S (2004) *Circulation* 109:2692–2697.
26. Hintze TH, Vatner SF (1984) *Circ Res* 54:50–57.
27. Sanderson WC, Scherbov S (2005) *Nature* 435:811–813.
28. Blackstone EH, Lytle BW (2000) *J Thorac Cardiovasc Surg* 119:1221–1230.

MEDICAL SCIENCES